Available online at www.ijpcr.com

International Journal of Pharmaceutical and Clinical Research 2016; 8(12): 1574-1582

ISSN- 0975 1556

Research Article

Enhanced Blood–Brain Barrier Transmigration Using the Novel Chrysin Embedded Solid Lipid Nanoformulation: A Salient Approach on Physico-Chemical Characterization, Pharmacokinetics and Biodistribution Studies

Aishwarya V, Sumathi T*

Department of Medical Biochemistry, Dr. ALM Post Graduate Institute of Basic Medical Sciences, University of Madras, Taramani Campus, Chennai – 600 113, Tamil Nadu, India.

Available Online: 25th December, 2016

ABSTRACT

Solid lipid nanoparticles are an alternative carrier system used to load the drug for targeting, to improve the bioavailability by increasing its solubility, and protecting the drug from presystemic metabolism. The present study aims at determining the physico-chemical characteristics, stability, *in-vivo* plasma pharmacokinetic and bio-distribution analysis of chrysin loaded solid lipid nanoparticles (CN-SLNs) for exploring the targeted brain delivery. FTIR spectra of CN-SLNs exhibited a possible chemical interaction between chrysin and the polymer matrix having the shift in the absorption peaks of C-O stretch and "oop" band C-H bend. Differential Scanning Calorimetric study of CN-SLNs showed the complete disappearance of the characteristic peak of chrysin which reveals that the drug is molecularly dispersed into the lipid. The stability study of CN-SLNs indicates the stability of the nanoformulations without changing its performance on storage for 6 months. Furthermore, the *in-vivo* pharmacokinetic study revealed that encapsulation of chrysin in solid lipid nanoparticles increased the oral bioavailability of chrysin to 5 folds when compared with that of free chrysin. In biodistribution studies, CN-SLNs could be detected in the evaluated organs, including liver, heart, spleen, lung, kidney and brain. Solid lipid nanoformulation significantly raised the chrysin concentration especially in the brain which emphasizes on the blood–brain barrier permeation. These findings thus provide further understanding for the possible therapeutic effects of CN-SLNs in further brain disorder related clinical research.

Keywords: Solid lipid nanoparticles, Chrysin, Brain drug delivery, Pharmacokinetics, Differential Scanning Calorimetry

INTRODUCTION

Brain drug delivery development remains challenging due to the tightness of the endothelial vascular lining, called blood–brain barrier (BBB), which represents the major obstacle for delivery of drugs to the brain[1,2]. Due to this difficulty, the development of a suitable non-invasive drug delivery system is required and hence a motivation for improving brain targeted drug delivery is vital to treat central nervous system disorders.

Flavonoids are plant polyphenolic compounds, which comprise several classes including flavonols, flavanones and flavanols. Chrysin (5,7-dihydroxyflavone) is a flavonoid that forms the main active component of the Indian trumpet tree (Oroxylum indicum)[3] and passion flower (Passiflora incarnata) as well as in edible items such as mushroom[4], honey[5]. Like other flavonoids, chrysin (CN) also exhibits various biological activities and pharmacological effects, including antioxidant[6], neuroprotective[7], anti-inflammatory[8], anti-hemolytic[9] and anti-hypertension[10] effects.

Although several studies has been reported that chrysin exhibits neuroprotective effect but its efficacy is often confined by the inability to pass the BBB. Most of the natural molecules were found to show compromised physiological properties and poor pharmacokinetics[11]. An efficient strategy to overcome the poor bioavailability of natural compounds, could be its inclusion in nanoparticles made from solid lipids, called solid lipid nanoparticles (SLNs). Various studies had reported that solid lipid nanoparticles (SLNs) can improve the ability of the drug to penetrate through the blood brain barrier and is a promising drug targeting system for the treatment of CNS disorders[12,13]. Moreover SLNs are taken up readily by the brain because of their lipidic nature and the bioacceptable and biodegradable nature of SLNs makes them less toxic as compared to polymeric nanoparticles[14]. SLNs offer unique properties such as small size, large surface area, high drug loading, the interaction of phases at the interfaces, and are attractive for their potential to improve performance of pharmaceuticals, neutraceuticals and other materials[15]. Advantages of SLNs are the use of physiological lipids, the avoidance of organic solvents in the preparation process, and a wide potential application spectrum (dermal, oral and intravenous). Additionally,

*Author for Correspondence: drsumathi.bioscience@gmail.com

improved bioavailability, protection of sensitive drug molecules from the environment (water, light) and controlled and/or targeted drug release[16,17,18], improved stability of pharmaceuticals, feasibilities of carrying both lipophilic and hydrophilic drugs and most lipids being biodegradable. SLNs possess a better stability and ease of upgradability to production scale as compared to liposomes. This property may be very important for many modes of targeting[19,20].

In our earlier study[21] of characterizing chrysin loaded solid lipid nanoparticles (CN-SLNs) showed a total drug content of 71.10 ± 3.12% and entrapment efficiency of 86.29 ± 3.42% with an average particle size of 240.0 ± 4.79 nm were prepared by hot homogenization followed by micro emulsion technique. Zeta potential studies confirmed the stability of the CN-SLNs preparation as indicated by the negative charge (-40.4 ± 2.54 mV) and the XRD studies showed reduced crystallinity. The in vitro release kinetics showed a maximum drug release of 88.80 ± 3.05% for CN-SLNs in 72 hrs, which ensures the controlled drug release property of CN-SLNs.

Although a few attempts have been made to formulate various drug delivery systems of chrysin-like nanoparticles[22,23,24], no prominent studies have been reported on enhancing the brain permeability of the drug. Accordingly, this investigation aimed to formulate solid lipid nanoparticles (SLNs) of CN for oral administration to improve its permeation across the blood–brain barrier into the central nervous system (CNS) and eventually, to improve its therapeutic efficacy in various CNS disorders.

MATERIALS AND METHODS

Chemicals and Reagents

Chrysin was obtained from Sigma Aldrich. Stearic acid, Lecithin and Sodium taurocholate were purchased from Hi-Media chemicals. All the other chemicals used in the present study were of analytical grade and purchased from Central Drug House Pvt. Ltd. and Sisco Research Laboratories Pvt. Ltd.

Preparation of Solid lipid nanoparticle encapsulated Chrysin (CN-SLNs)

The SLNs preparation technique was previously published by our group according to Frautschy SA and Cole GM (2009) method[25], with slight modifications. Briefly, stearic acid mole fraction 0.710, lecithin mole fraction 0.210, taurocholate mole fraction 0.069 and CN mole fraction 0.011 were used to produce the Solid lipid nanoparticles encapsulated CN. Stearic acid was maintained at ~75 °C to melt completely, simultaneously distilled water was heated up to ~75 °C in a separate beaker. Typically, surfactants were added to distilled water on a magnetic stirrer and allowed to equilibrate at ~75 °C. The water-surfactant solution containing CN was then added to the melted lipid and again allowed to equilibrate at ~75 °C. The mixture was then homogenized at 24,000 rpm for 150 s to form the emulsion. Then the aliquot was continuously stirred near ice cold water (~2 °C), at a ratio of 1:20 (warm microemulsion/cold water) resulting in the formation of solidified solid lipid nanoparticles. The final product was centrifuged at 20,000×g for 15 min, and nanoparticle pellet was resuspended in distilled water. The preparation was stored in a sterile vial at 4 °C, until use.

Formulation characterization

Fourier-transform infrared (FTIR) spectroscopic study

FTIR spectroscopy measurements were used to investigate the possible chemical interactions between chysin and the polymer matrix. The spectrum was recorded for CN-SLNs, CN, SLNs and stearic acid using Spectrum BX infrared spectrophotometer[26]. Samples were prepared in KBr disk (2 mg sample in 200 mg KBr) with a hydrostatic press at a force of 40 psi for 4 min. The scanning range employed was 400–4000 cm^{-1} at a resolution of 4 cm^{-1}.

Differential Scanning Calorimetry (DSC) analysis

DSC analysis of stearic acid, SLNs, CN and CN-SLNs to evaluate any possible physical interaction. For DSC measurement, 10 mg of samples was put in an open aluminium pan, and then heated at the scanning rate of 10°C/min between 0 and 400°C temperature range under a dry nitrogen atmosphere. Empty aluminum pans were used as standard reference material to calibrate the temperature and energy scale of the DSC apparatus, the entire thermal behavior was studied under a nitrogen purge[27].

Stability studies

CN-SLNs dispersion was stored at refrigerated temperature (2-8°C) for 6 months under a sealed condition. The average particle size, in-vitro drug release property and physical characteristics were determined periodically after 1, 3 and 6 months[28].

In-vivo pharmacokinetic studies

Adult male Sprague-Dawley rats weighing 250-300 g were obtained from the Central Animal House, Dr. ALMPGIBMS, University of Madras, Tamil Nadu, India. Rats were housed separately in polypropylene cages and fed a standard pellet diet, kept under hygienic conditions. Rats were kept on a 12 h light and dark cycles with free access to water. All experiments and protocols described in the present study were approved by the Institutional Animal Ethics Committee (IAEC) (IAEC No: 01/02/2015) of Dr. ALMPGIBMS, University of Madras. The in-vivo pharmacokinetic studies were carried out with 12 male Sprague-Dawley rats divided randomly into 2 groups with 6 animals each. The first group was orally administered a single dose of CN-SLNs (20 mg/kg). To another group, CN suspension (20 mg/kg) (CN dispersed in 2% dimethyl sulfoxide) was administered to obtain a contrast pharmacokinetic behavior with a conventional formulation. 1mL of blood was withdrawn from the retro-orbital plexus under light ether anesthesia at specified time intervals (pre-dose, 0.5, 1, 2, 4, 6, 8, 10, 12, 18, 24 h), into heparinized tubes and immediately centrifuged at 3000 rpm for 15mins. After centrifugation, the plasma obtained was analyzed spectrophotometrically for the concentration of chrysin[29].

Biodistribution analysis

Healthy male Sprague-Dawley rats were randomly divided into 2 groups of 11 animals each. For each group, a single dose of the formulation CN-SLNs and CN suspension was administered. After various time intervals (pre-dose, 0.5, 1, 2, 4, 6, 8, 10, 12, 18, 24 h), organs viz. brain, heart, lungs, liver, spleen and kidneys were immediately

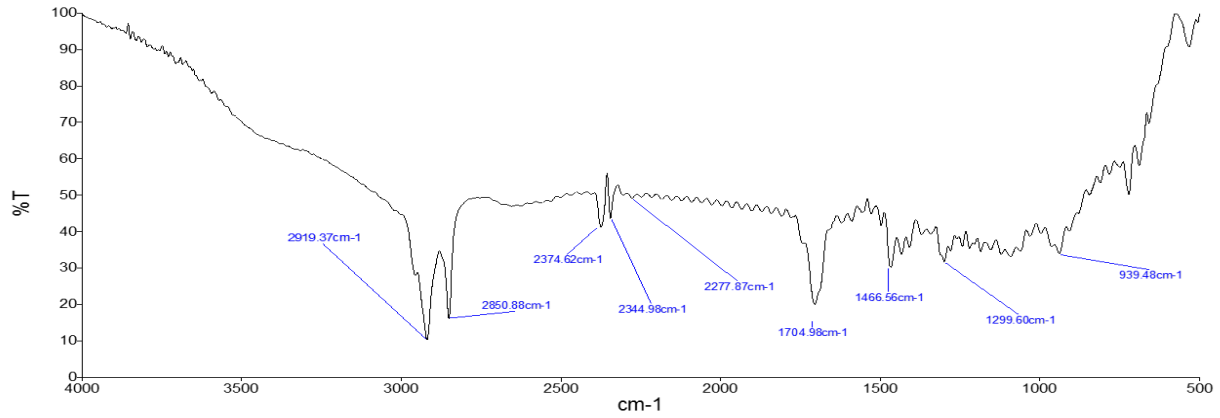

a

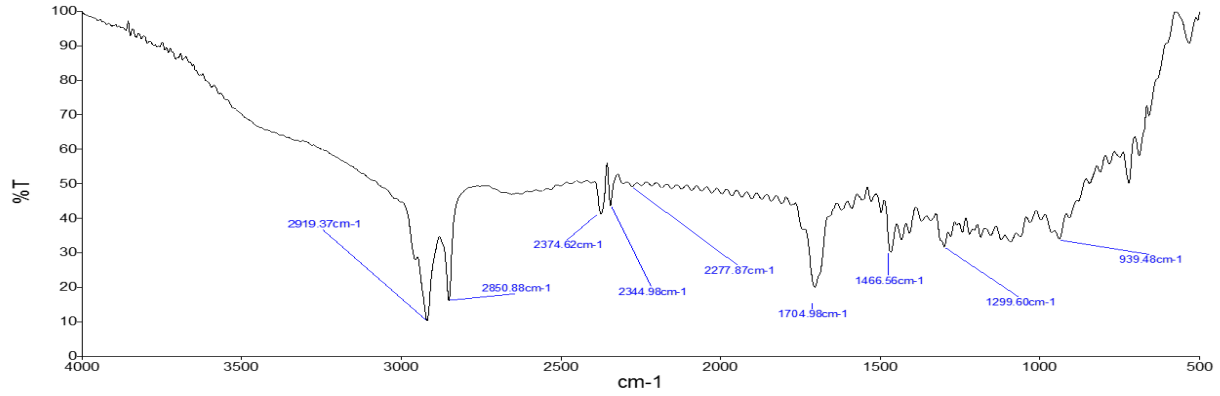

b

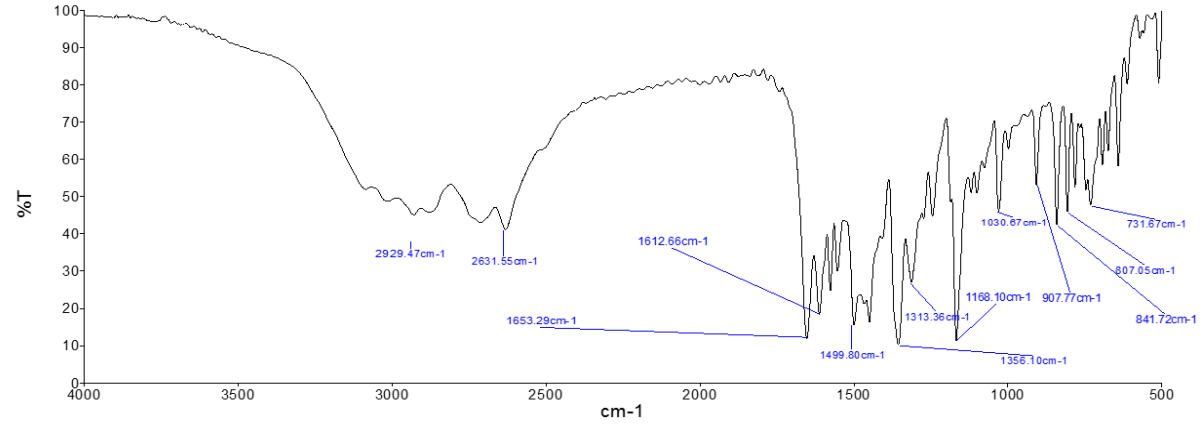

c

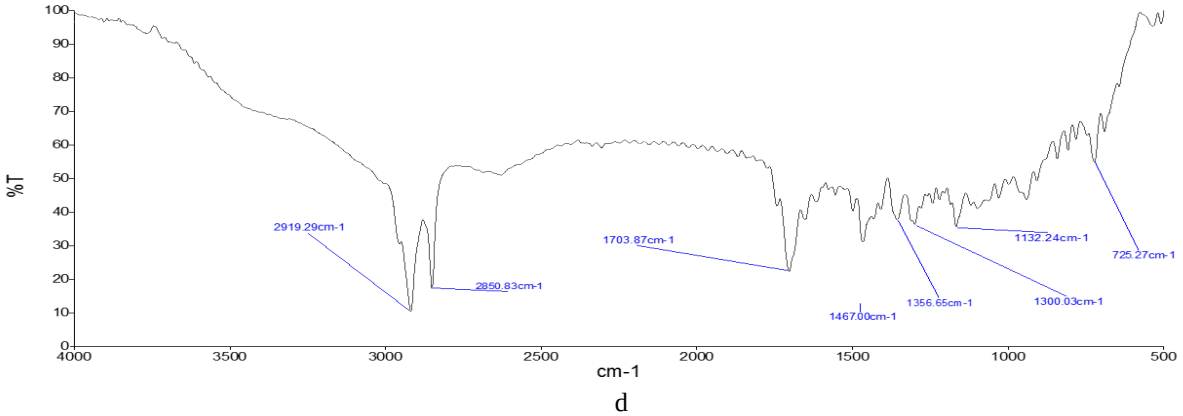

d

Figure 1: (a) FTIR spectrum of Stearic acid, (b) B-SLNs, (c) CN and (d) CN-SLNs.

removed from each group and subjected to homogenization by adding 1mL ice-cold KCl solution per 0.5 g tissue. The supernatant obtained was analyzed spectrophotometrically for chrysin concentration[29].

Statistical analysis

Data represents mean ± S.D. Statistical comparisons were performed by one way analysis of variance (ANOVA) followed by Tukey's test. A value of $P<0.05$ was considered as statistically significant.

RESULTS

FT-IR spectroscopic analysis

FT-IR spectroscopy was employed to obtain conformational information about the lipid molecules and it is used to investigate the interactions between lipid, drug and other excipients. Fig.1. shows the FT-IR spectra of the stearic acid, blank SLNs (B-SLNs), CN and CN-SLNs. The IR spectrum of stearic acid (Fig. 1a) showed the absorption bands of 2918.24 cm^{-1}, 2850.03 cm^{-1} (C-H stretch), 1700.38 cm^{-1} (C=O stretch), 1432.7 cm^{-1}, 941.66 cm^{-1} (O-H bend) and 1297.80 cm^{-1} (C-O stretch). The IR spectrum of B-SLNs (Fig. 1b) showed the characteristic absorption peaks of stearic acid at 2919.37 cm^{-1}, 2850.88 cm^{-1} (C-H stretch), 1704.08 cm^{-1} (C=O stretch), 1466.56 cm^{-1} (C-C stretch in-ring), 1299.60 cm^{-1} (C-O stretch) and 939.48 cm^{-1} (C-H in-plane bend). The IR spectrum of CN (Fig. 1c) showed the absorption bands of 2929.47 cm^{-1} (C-H stretch), 2631.55 cm^{-1} (O-H stretch), 1653.29 cm^{-1}, 1612.66 cm^{-1} (C-C=C symmetric stretch), 1499.80 cm^{-1} (C-C=C asymmetric stretch), 1168.10 cm^{-1}, 1030.61 cm^{-1} (C-O stretch), 907.77 cm^{-1}, 841.72 cm^{-1}, 807.05 cm^{-1}, 731.67 cm^{-1} ("oop" band C-H bend). The IR spectrum of CN-SLNs (Fig. 1c) recorded the characteristic absorption bands of stearic acid and CN. The C-O stretching and "oop" band C-H bend frequency of chrysin appears at 1168.10 cm^{-1} and 731.67 cm^{-1} respectively. After adsorption these peaks disappears. Instead bands at 1132.24 cm^{-1} and 725.27 cm^{-1} appears. This shows the shift in the C-O stretch and "oop" band C-H bend which can be interpreted as possible interaction between the drug and the lipid carrier.

Differential scanning calorimetry (DSC)

DSC analysis was carried out in order to identify possible interactions between the components. Fig.2. shows the DSC thermogram of stearic acid, B-SLNs, CN and CN-SLNs. The DSC curve for physical mixture of lipid (Stearic acid) showed the presence of endothermic peaks at 73.6°C with a enthalpy change at 215.8 J/g (Fig.2a). DSC thermogram of B-SLNs (Fig.2b) exhibits an endothermic peak at 68.4°C with an enthalpy change at 114.1 J/g. In Fig.2c CN showed a sharp endothermic peak at 290.5°C with an enthalpy change at 151 J/g, due to its crystalline nature. On the other hand, the thermogram of CN-SLNs in fig.2d did not show the endothermic peak for CN, but it shows the characteristic peak of the surfactant at 68.3°C with an enthalpy change at 134 J/g with minimum shifting. This suggests that CN present in the nanoformulation was not in crystalline state but in amorphous state or molecularly dispersed structure of the drug in lipid matrix. These results are consistent with previous studies reported by Rahul Nair et.al.[30]

Stability analysis

The physical stability of CN-SLNs and CN was evaluated for 6 months at time intervals of 0^{th}, 3^{rd} and 6^{th} month. Table. 1 shows the physico-chemical characteristics of CN-SLNs and CN. The refrigerated CN-SLNs samples has a maximum particle size of 248.5±6.01 nm and the zeta potential of -30.72±2.34 at 6^{th} month. Further, the stored CN-SLNs also observed to be opalescent during the period of 6 months and the pH was found to 7.01±0.04. The drug content and encapsulation efficiency were also assessed, where the results showed no significant changes during the storage for a period of 6 months. The in-vitro drug release of the stored nanoformulation showed the maximum drug release of 83.19% at a period of 72 hr. Furthermore, the free CN during the storage of 6 months turned into turbid with a pH of 8.31±0.12. Also, the percentage of drug encapsulation and in-vitro drug release property were reduced during the storage period. From the results it can be concluded that CN-SLNs showed a stable physico-chemical properties over a period of 6 months. Being hydrophilic polymer SLNs acts as a coat to shield the particle surface charge responsible to cause their

Table 1: Stability evaluation of CN-SLNs and CN for its physico-chemical characteristics.

Stability tests	CN-SLNs			CN		
Period (month)	0	3	6	0	3	6
Sample clarity	Opalescent	Opalescent	Opalescent	Clear	Turbid	Turbid
Sediment formation	No	No	No	No	Yes	Yes
pH ± SD	7.00±0.03	7.02±0.06	7.01±0.04	7.07±0.06	7.47±0.08	8.31±0.12
Particle size ± SE(nm)	240.0±6.92	244.6±5.68	248.5±6.01	1358±5.13	1562±7.87	1775±6.08
PDI ± SE	0.285±0.03	0.331±0.04	0.365±0.02	0.802±0.26	0.855±0.19	0.912±0.29
Maximum drug release in 72h ± SE (%)	88.29±3.42	85.74±2.74	83.19±3.38	41.87±4.12	37.52±3.55	32.94±4.06

Stability tests are represented as mean ± SD/SE (n=3).

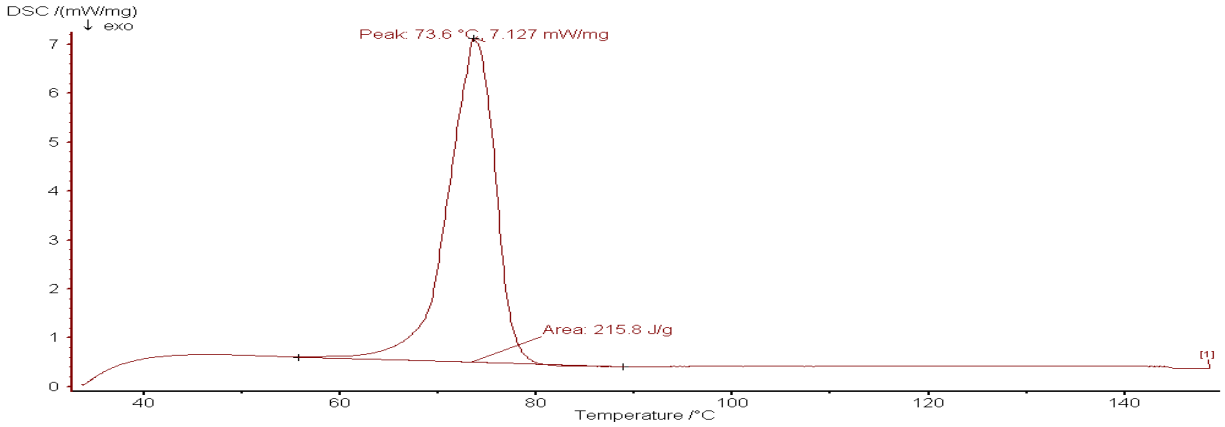

a

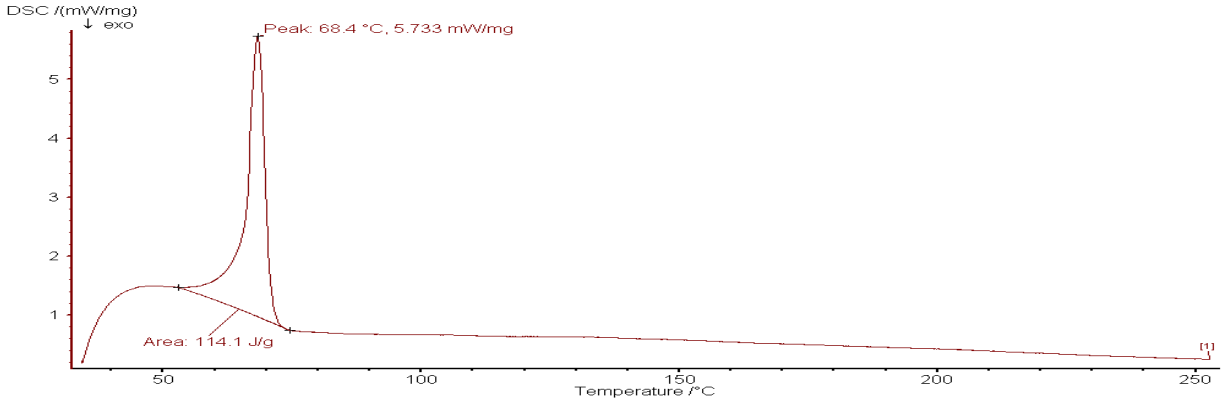

b

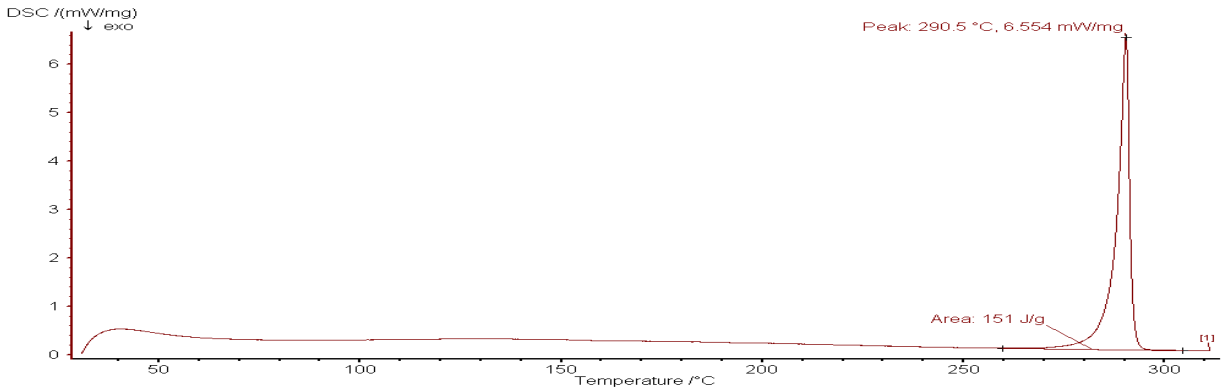

c

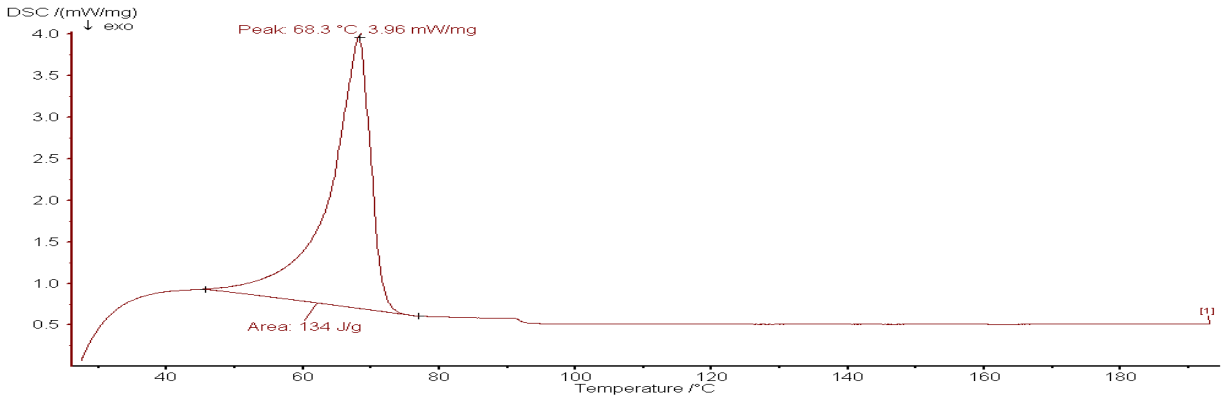

d

Figure 2: (a) DSC thermogram of Stearic acid, (b) B-SLNs, (c) CN and (d) CN-SLNs.

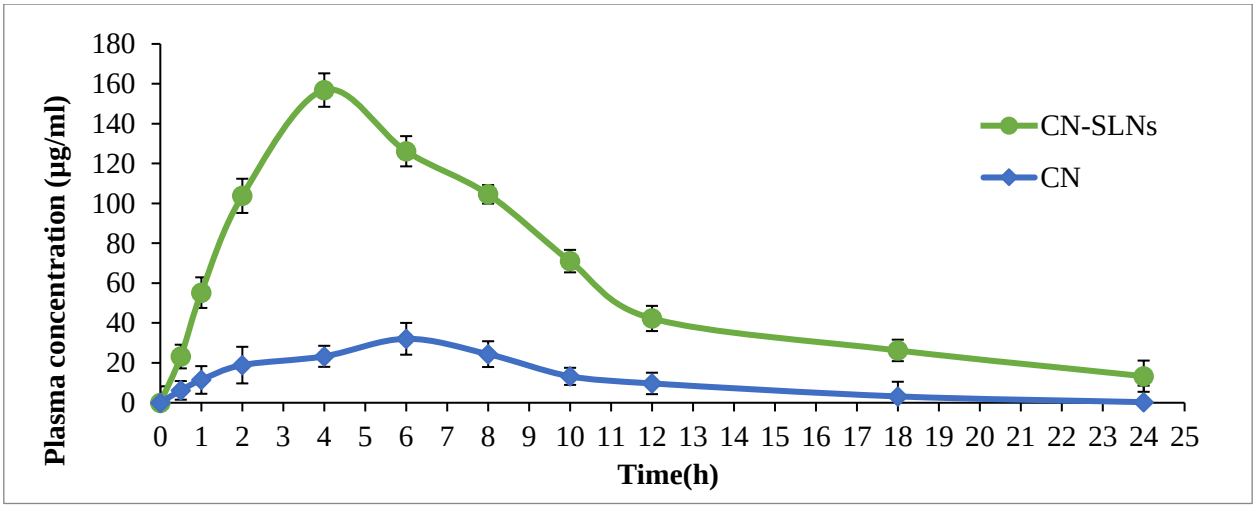

Figure 3: Plasma pharmacokinetic profile of CN-SLNs and CN at various time periods.

Table 2: Pharmacokinetics parameters of CN-SLNs and CN.

Pharmacokinetic Profiles	CN-SLNs	CN
$AUC_{0-\infty}$ (µg/ml/h)	2187.199 ± 116.275 [a]	428.479 ± 24.384
C_{max} (µg/ml)	156.856 ± 8.39 [a]	32.076 ± 7.98
T_{max} (h)	4	6
Ke (h^{-1})	0.113 ± 0.05	0.397 ± 0.04
Vd (L)	0.079 ± 0.03	0.118 ± 0.07
$t_{1/2}$ (h)	6.132 ± 0.19 [a]	1.745 ± 0.16
CL_{total} (Lh^{-1})	0.009 ± 0.008	0.047 ± 0.013

agglomeration and can easily compensate for the missing electrostatic repulsion and stabilize the dispersion for a longer time[31]. Thus, SLNs nanoformulation contributes for the stability of CN by its protective nature.

Plasma pharmacokinetic profile

Chrysin loaded SLNs were designed in order to improve poor bioavailability associated with CN, a drug with tremendous therapeutic potential. Plasma levels of CN-SLNs after administration were compared with those attained after administration of free CN. Negligible plasma levels were attained after administration of free CN. Encapsulation of CN into SLNs led to 5 fold increase in bioavailability. The relative pharmacokinetic parameters including area under the concentration-time curve from zero to infinity ($AUC_{0-\infty}$), maximum concentration achieved in the blood (C_{max}), time needed to reach maximum concentration (T_{max}), elimination rate constant (Ke), volume of distribution (Vd), elimination half-life ($t_{1/2}$) and total clearance (CL_{total}) are listed in table 2.

Pharmacokinetic parameters are represented as mean ± SD (n=6). [a]$P<0.05$ shows statistically significant compared to free CN administered group. $AUC_{0-\infty}$ – Area under the concentration-time curve from zero to infinity; C_{max} – Maximum concentration achieved in the blood; T_{max} – Time needed to reach maximum concentration; Ke – Elimination rate constant; Vd – Volume of distribution; $t_{1/2}$ – Elimination half-life; CL_{total} – Total clearance.

Distribution studies in brain and other tissues

Biodistribution profiles of CN-SLNs and free CN in brain, heart, kidneys, liver, lungs, and spleen are depicted in Fig. 4. A whole biodistribution study of CN-SLNs formulations during 24h was performed giving information about the potentiality of SLN formulations for targeting incorporated drugs to the brain. Results revealed remarkable differences between CN-SLNs and CN. As previously reported, nanoparticles could significantly change the body distribution of the incorporated drugs[32,33,34,35]. CN distribution after administration indicated that CN concentration increased remarkably in brain when CN was incorporated in SLNs. The CN-SLNs nanoformulation was distributed mainly to the brain ($AUC_{0\rightarrow\infty}$ 75.3645±1.374 µg/g/h) followed by liver ($AUC_{0\rightarrow\infty}$ 19.0311±2.036 µg/g/h), kidney ($AUC_{0\rightarrow\infty}$ 13.4119±1.813 µg/g/h), heart ($AUC_{0\rightarrow\infty}$ 11.8531± 2.822 µg/g/h), spleen ($AUC_{0\rightarrow\infty}$ 9.8603±2.938µg/g/h) and lung ($AUC_{0\rightarrow\infty}$ 2.0358± 3.107 µg/g/h). The biodistribution pattern strongly supports the existence of CN in intact form within the lipid carrier which would allow the drug to cross the BBB.

CONCLUSION

Enhancement of drug uptake into brain is a delicate task in the treatment of several neurological disorders. In the present study, the results were remarkably emphasized on the high accumulation of CN-SLNs in the brain tissue compared with other organs suggesting the targeting potential of SLNs on BBB permeation. Therefore, SLN was demonstrated to be a promising nano carrier for targeting CN to the brain as it possessed with remarkable biocompatibility, stability and efficacy than other delivery systems. Thus, CN-SLNs with enhanced BBB permeation can form a therapeutic armamentarium for various brain diseases.

ACKNOWLEDGEMENT

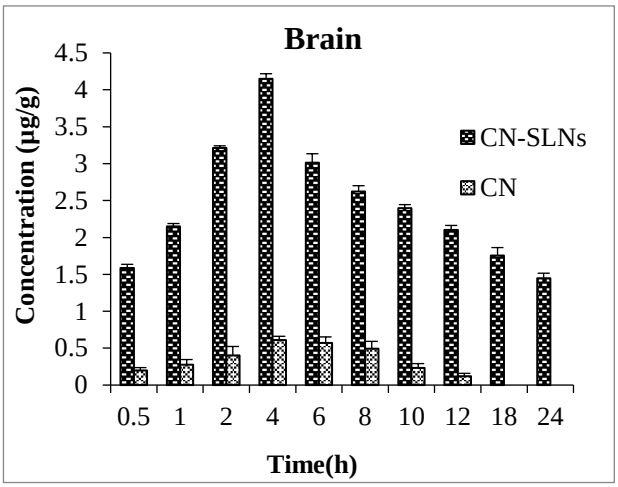

a

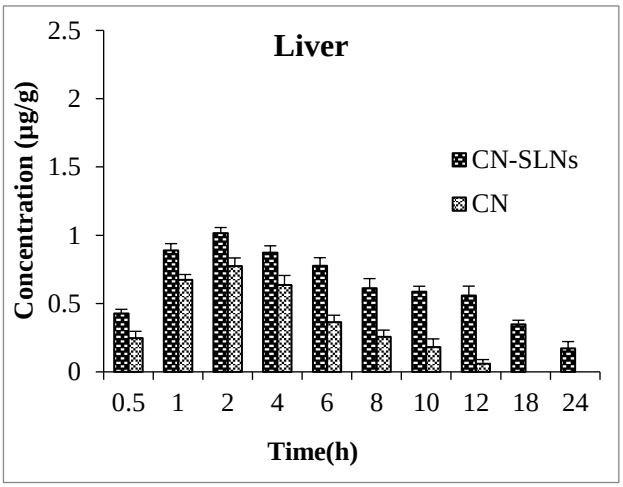

b

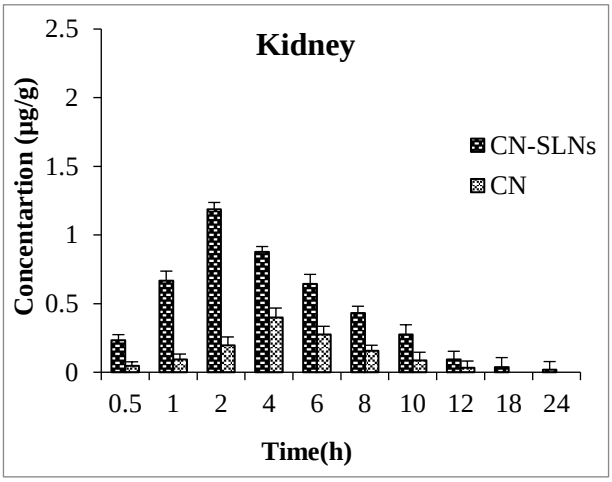

c

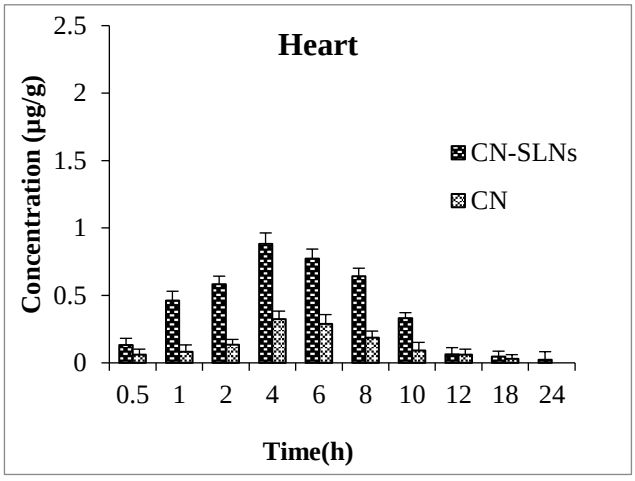

d

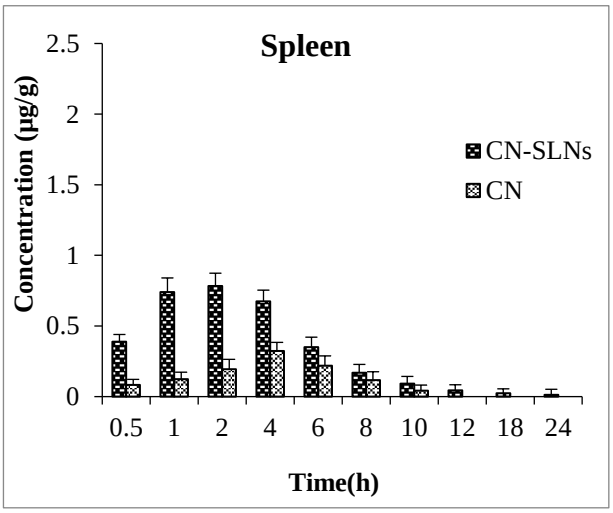

e

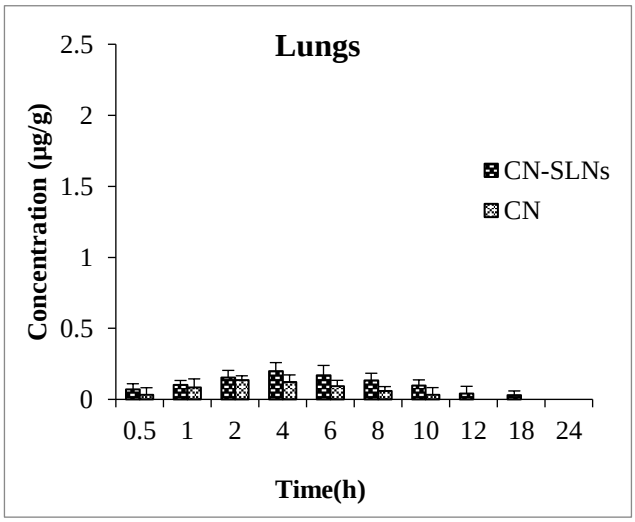

f

Figure 4 (a-f): Tissue distributions of CN-SLNs and CN at various time periods.

The first author is grateful to UGC for the financial support in the form of JRF – UGC – BSR Fellowship. And also, the authors thank **"**Sophisticated analytical instrument facility (SAIF), Indian Institute of Technology-Madras, India" for providing Differential scanning calorimetry facility to perform the thermal behavior of nanoformulation.

REFERENCES

1. Pardridge WM. Alzheimer's disease drug development and the problem of the blood–brain barrier. Alzheimer's Dement. 2009; 5:427–432.
2. Abbott NJ, Patabendige AAK, Dolman DEM, Yusof SR, Begley DJ. Structureand function of the blood–brain barrier. Neurobiol Dis. 2010; 37:13–25.
3. Zhang G, Chen X, Guo J, Wang J. Spectroscopic investigation of the interaction between chrysin and bovine serum albumin. J Mol Struct. 2009; 921:346–351.
4. Jayakumar T, Thomas PA, Geraldine P. In-vitro antioxidant activities of an ethanolic extract of the oyster mushroom, Pleurotus ostreatus. Innov Food Sci Emerg Technol. 2009; 10:228-34.
5. Williams CA, Harborne JB, Newman M, Greenham J, Eagles J. Chrysin and other leaf exudate flavonoids in the genus Pelargonium. Phytochemistry. 1997; 46:1349-53.
6. Bors W, Michael C, Stettmaier K. Antioxidant effect of flavonoids. Biofactors. 1997; 6:399-402.
7. Thangarajan S, Ramachandran S, Krishnamurthy P. Chrysin exerts neuroprotective effects against 3-Nitropropionic acid induced behavioral despair-Mitochondrial dysfunction and striatal apoptosis via upregulating Bcl-2 gene and downregulating Bax-Bad genes in male wistar rats. Biomed Pharmacother. 2016; 84:514-525.
8. Lin YL, Lin JK. (2)-Epigallocatechin-3-gallate Blocks the Induction of Nitric Oxide Synthase by Down-Regulating Lipopolysaccharide-Induced Activity of Transcription Factor Nuclear Factor-kB. Mol Pharmacol. 1997; 52:465–472.
9. Chaudhuri S, Banerjee A, Basu K, Sengupta B, Sengupta PK. Interaction of flavonoids with red blood cell membrane lipids and proteins: antioxidant and antihemolytic effects. Int J Biol Macromol. 2006; 41:42–48.
10. Fishkin RJ, Winslow JT. Endotoxin-induced reduction of social investigation by mice: interaction with amphetamine and anti-inflammatory drugs. Psychopharmacology (Berl). 1997; 132:335–341.
11. Rubió L, Macià A, Motilva MJ. Impact of various factors on pharmacokinetics of bioactive polyphenols: an overview. Curr Drug Metab. 2014; 15(1):62-76.
12. Blasi P, Giovagnoli S, Schoubben A, Ricci M, Rossi C. Solid lipid nanoparticles for targeted brain drug delivery. Adv Drug Deliv Rev. 2007; 59(6):454-477.
13. Medha Patel, Eliana B Souto, Kamalinder K Singh. Advances in brain drug targeting and delivery: limitations and challenges of solid lipid nanoparticles. Expert Opin Drug Deliv. 2013; 10(7):889-905.
14. Kaur IP, Bhandari R, Bhandari S, Kakkar V. Potential of solid lipid nanoparticles in brain targeting. J Control Release. 2008; 127(2):97-109.
15. Cavalli R, Caputo O, Gasco MR. Solid lipospheres of doxorubicin and idarubicin. Int J Pharm. 1993; 89(1):R9–R12.
16. Mehnert W, Mäder K. Solid lipid nanoparticles: production, characterization and applications. Adv Drug Deliver Rev. 2001; 47(2–3):165–196.
17. Muller RH, Olbrich C, Kayser O. Lipase degradation of Dynasan 114 and 116 solid lipid nanoparticles (SLN) – effect of surfactants, storage time and crystallinity. Int J Pharm. 2002; 237:119–128.
18. Muller RH, Maader K, Gohla S. Solid lipid nanoparticle (SLN) for controlled drug delivery-review of the state of the art. Eur J Pharm Biopharm. 2000; 50:161–177.
19. Muller RH, Runge SA. Solid lipid nanoparticles (SLN) for controlled drug delivery. In Submicron Emulsions in Drug Targeting and Delivery. Edited by Benita S. Amsterdam: Harwood Academic Publishers. 1998; 219–234.
20. Jenning V, Gysler A, Schafer-Korting M, Gohla S. Vitamin A loaded solid lipid nanoparticles for topical use: occlusive properties and drug targeting to the upper skin. Eur J Pharm Biopharm. 2000; 49(3):211–218.
21. Aishwarya V, Surekha R, Sumathi T. Preparation, Characterization and In-Vitro Cell Viability assay of Chrysin loaded Solid Lipid Nanoparticles as Drug Delivery System. Int J Pharm Bio Sci. 2015; 6(1):465 – 478.
22. Chakraborty S, Basu S, Lahiri A, Basak S. Inclusion of chrysin in b-cyclodextrin nanocavity and its effect on antioxidant potential of chrysin: A spectroscopic and molecular modeling approach. J Mol Struct. 2010; 977:180–188.
23. Zheng H, Li S, Pu Y, Lai Y, He B, Gu Z. Nanoparticles generated by PEG-Chrysin conjugates for efficient anticancer drug delivery. Eur J Pharm Biopharm. 2014; 87:454–460.
24. Mohammadinejad S, Akbarzadeh A, Rahmati-Yamchi M, Hatam S, Kachalaki S, Zohreh S, Zarghami N. Preparation and Evaluation of Chrysin Encapsulated in PLGA-PEG Nanoparticles inn T47-D Breast Cancer Cells. Asian Pac J Cancer Prev, 2015; 16 (9):3753-3758.
25. Frautschy SA, Cole GM. Bioavailable curcuminoid formulations for treating Alzheimer's disease and other age-related disorders. United States, US: 2009/0324703 A1, 2009.
26. Madan J, Pandey RS, Jain V, Katare OP, Chandra R, Katyal A. Poly (ethylene)-glycol conjugated solid lipid nanoparticles of noscapine improve biological half-life, brain delivery and efficacy in glioblastoma cells. Nanomedicine. 2013; 9:492–503.
27. Dodiya SS, Chavhan SS, Sawant KK, Korde AG. Solid lipid nanoparticles and nanosuspension formulation of Saquinavir: preparation, characterization, pharmacokinetics and biodistribution studies. J Microencapsul. 2011; 28(6):515–527.
28. Venishetty VK, Samala R, Komuravelli R, Kuncha M, Sistla R, Diwan PV. β-Hydroxybutyric acid grafted solid lipid nanoparticles: A novel strategy to improve drug delivery to brain. Nanomedicine. 2013; 9:388–397.
29. Miniati E. Assessment of phenolic compounds in biological samples. Ann Ist Super Sanità. 2007; 43(4):362-368.

30. Rahul Nair, Arun Kumar KS, Vishnu Priya K, Md. Badivaddin T, Sevukarajan M. Preparation and characterization of Rizatriptan loaded solid lipid nanoparticles. J Biomed Sci and Res. 2011; 3(2):392-396.
31. Joshi AS, Patel HS, Belgamwar VS, Agrawal A, Tekade AR. Solid lipid nanoparticles of ondansetron HCl for intranasal delivery: development, optimization and evaluation. J Mater Sci Mater Med. 2012; 23(9):2163-2175.
32. Botella P, Abasolo I, Fernández Y, Muniesa C, Miranda S, Quesada M, Ruiz J, Schwartz S Jr, Corma A, Surface-modified silica nanoparticles for tumor-targeted delivery of camptothecin and its biological evaluation. J Control Release. 2011; 156:246–257.
33. Bondì ML, Craparo EF, Giammona G, Drago F. Brain-targeted solid lipid nanoparticles containing riluzole: preparation, characterization and biodistribution. Nanomedicine (Lond). 2010; 5(1):25-32.
34. Yang S, Zhu J, Lu Y, Liang B, Yang C. Body distribution of camptothecin solid lipid nanoparticles after oral administration. Pharm Res. 1999; 16:751–757.
35. Yang SC, Lu LF, Cai Y, Zhu JB, Liang BW, Yang CZ. Body distribution in mice of intravenously injected camptothecin solid lipid nanoparticles and targeting effect on brain. J Control Release. 1999; 59:299–307.